Thermal and Mechanical Properties of LDPE/Sisal Fiber Composites Compatibilized with Functionalized Paraffin Waxes

L. P. Nhlapo, A. S. Luyt

Department of Chemistry, University of the Free State (Qwaqwa Campus), Phuthaditjhaba 9866, South Africa

Received 24 August 2010; accepted 26 May 2011
DOI 10.1002/app.35023
Published online 22 September 2011 in Wiley Online Library (wileyonlinelibrary.com).

ABSTRACT: The effect of maleic anhydride-grafted hard paraffin wax (MA-*g*-wax) and oxidized hard paraffin wax (OxWax), as possible compatibilizers, on the morphology, thermal and mechanical properties of LDPE/sisal fiber composites were examined. The differential scanning calorimetry (DSC) results show that sisal alone did not change the crystallization behavior of LDPE, while the two waxes influenced the crystallization behavior of LDPE in different ways, whether mixed with LDPE alone or in the presence of sisal. The thermal properties seem to be influenced by the fact that the waxes preferably crystallize around the short sisal fibers, and by the fact that the two waxes have different compatibilities with LDPE. The TGA results show an increase in the thermal stability of the blends in the presence of the two waxes, with LDPE/OxWax showing a more significant improvement. The presence of wax, however, reduced the thermal stability of the LDPE/sisal/wax composites. The presence of OxWax and MA-*g*-wax similarly influenced the tensile properties of the composites. Both waxes similarly improved the modulus of the compatibilized composites, but in both cases the tensile strengths were worse, probably because of a fairly weak interaction between LDPE and the respective waxes. © 2011 Wiley Periodicals, Inc. J Appl Polym Sci 123: 3627–3634, 2012

Key words: composites; LDPE; sisal fiber; functionalized waxes; morphology; properties

INTRODUCTION

The incorporation of natural fibers into a polymer commonly leads to significant changes in the mechanical properties of the composites. However, a problem encountered when trying to combine natural fibers with thermoplastic materials like polyolefins is one of incompatibility due to the hydrophilic nature of the natural fibers. Therefore, the use of a compatibilizer or coupling agent, which alleviates gross segregation and promotes adhesion, is necessary to reduce the interfacial tension between the hydrophobic polyolefins and the hydrophilic natural fibers. The choice of compatibilizers or coupling agents is critical for optimizing the dispersion and properties of the polyolefins. Besides, a good compatibilizer should provide stronger adhesion between the natural fibers and the polymer, and form entanglements and/or segmental crystallization with the polymeric matrix. The polymeric compatibilizer is expected to be compatible with the matrix material, as morphology has a significant effect on the polymer properties.

Correspondence to: A. S. Luyt (LuytAS@qwa.ufs.ac.za).

Journal of Applied Polymer Science, Vol. 123, 3627–3634 (2012)

Different techniques have been used to prepare polyolefin/natural fiber composites. These techniques include solution mixing, roll milling, melt mixing, as well as injection and compression molding.[1–12] The methods differ in terms of their operating principles and processing parameters, which may lead to fairly different properties of the prepared composite materials. Polyolefin/natural fiber composites were generally pretreated on the surface of the fiber or incorporated with surface modifiers to improve the interfacial adhesion between the hydrophilic natural fibers and the hydrophobic polyolefins. This can be achieved by using treatments such as silane coupling agents, compatibilizers, maleated polyolefins (maleic anhydride grafted polypropylene or maleic anhydride grafted polyethylene), as well as alkali and radiation treatments.[1,2,8,13]

Many studies focused on the preparation and morphology of non-treated composites. Colom et al.[7] and Mengeloglu et al.[15] focused on non-treated HDPE/wood fiber composites. They found poor adhesion between the non-polar HDPE matrix and the polar wood fiber, and inadequate wetting of the non-treated fibers within the HDPE matrix. They related these to the presence of large numbers of voids between the HDPE matrix and the wood fiber, and fiber-pull-out producing holes with smooth walls in the polymer matrix. The SEM results, in all

cases, showed that non-treated fibers appeared to be free of any matrix adhering to them.[5] However, Li et al.[13,15] reported that some parts of the wood fiber were covered with the polymer due to mechanical interlocking. Herrera-Franco et al.,[11] Albano et al.,[4] and Mohanty et al.[12] investigated composites based on HDPE and henequen fiber, seaweed residues, and jute fibers. The SEM results revealed poor interfacial adhesion between the components in the non-treated composites due to poor interfacial adhesion.

A number of studies reported on LDPE reinforced with natural fibers. Torres et al.[16] and Joseph et al.[17] used sisal fiber, whereas Kaci et al.[18] used oil husk flour to reinforce LDPE. The composites were prepared through compression molding, melt mixing, and solution mixing. The SEM results in all the studies showed relatively large gaps, fiber pull out and no coating on the surfaces of the fibers. Oksman et al.[19] and Freire et al.[20] used wood fibers to reinforce an LDPE matrix. In both cases the composites were prepared through injection molding. Again the SEM results in all cases showed poor interfacial adhesion between the wood fibers and the LDPE matrix.

Coupled polyolefin/natural fiber composites showed improved properties related to the morphology. The coupling was done on either the fiber surface or through polymer treatment. These provided enhanced interfacial adhesion between the polymer matrix and the fiber, good fiber dispersion within the matrix, and good fiber coating by the polymer. The degree of interfacial adhesion of the composite components was shown to depend largely on the chemical nature of the chosen coupling agent.[21] Various coupling agents such as wax, silane, organosilanes, maleic anhydride, maleic anhydride grafted polyolefins, acrylic acid grafted polyolefins, organic peroxides, ethylene-vinyl alcohol copolymers, and poly(ethylene-*co*-vinyl acetate) were used to enhance the compatibility between the natural fibers and the polyolefins.[2,22–28] Through the application of these coupling agents good compatibility and interfacial adhesion between the polyolefin matrices and the various natural fibers were achieved. The SEM results generally showed the absence of gaps between the fibers and the matrices, reduction in fiber pull-out resulting in small voids and few cavities, improved fiber dispersion in the polymer matrices, good fiber covering by the polymers and less fiber agglomeration.

The incorporation of natural fibers into a polymer is known to cause substantial changes in the mechanical properties of the composites. The quality of the fiber–matrix interface is important for the application of natural fibers as reinforcement for polymers. Because the fibers and matrices are chemically different, strong adhesion at their interfaces is needed for an effective stress transfer and bond distribution throughout the interface. The mechanism of reinforcement is dependent on the stress transfer between the matrix material and the embedded fiber. In particular, the fiber–matrix interfacial shear strength is one of the important parameters in controlling the toughness and the strength of a composite material. Its value is particularly dependent on fiber surface treatment, modification of the matrix, and other factors affecting the properties of the fiber–matrix interface.[17,29–32]

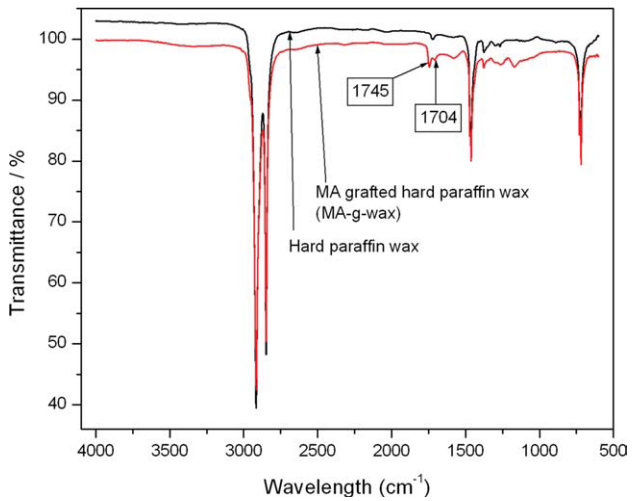

Figure 1 FTIR spectra for an unmodified Fischer-Tropsch wax, and the same wax grafted with 5 wt % MA. [Color figure can be viewed in the online issue, which is available at wileyonlinelibrary.com.]

EXPERIMENTAL

Materials

Oxidized Fischer-Tropsch paraffin wax (OxWax) is an oxidized straight-hydrocarbon chain paraffin wax with an average molar mass of 660 g mol^{-1}, a density of 0.95 g cm^{-3} (solid), and 0.82 cm^{-3} (liquid) at 25 and 110°C respectively, and a melting point of 96°C. It has a thermal decomposition temperature of about 250°C, C/O ratio of 18.8 : 1, and a flash point of $\sim$ 185°C. A hard Fischer-Tropsch paraffin wax (T_m = 90°C, ρ = 0.94 g cm^{-3}, average M_w = 785 g mol^{-1}) was used to prepare the maleic anhydride (MA) grafted wax (MA-*g*-wax). Both waxes were supplied by Sasol Wax, Sasolburg, South Africa. The MA grafting of the wax is described in a previous paper from our group.[33] The Fourier-transform infrared (FTIR) spectra in Figure 1 confirm the presence of functional groups on the chains of MA-*g*-wax. The wavenumbers of interest are 1704 cm^{-1} (characteristic of carbonyl from carboxylic dimmer acids) and 1745 cm^{-1} (characteristic of five-membered cyclic anhydride carbonyls).[34]

TABLE I
Compositions of Samples Investigated in this Study

LDPE/ MA-*g*-wax blends (w/w)	LDPE/OxWax blends (w/w)	LDPE/sisal/ MA-*g*-wax composites (w/w)	LDPE/sisal/ OxWax composites (w/w)	LDPE/sisal composites (w/w)
100/0/0	100/0/0	100/0/0	100/0/0	100/0/0
95/5	95/5	85/10/5	85/20/5	90/10
90/10	90/10	80/10/10	80/10/10	80/20
–	–	75/20/5	75/20/5	70/30
–	–	70/20/10	70/20/10	–
–	–	65/30/5	65/30/5	–
–	–	60/30/10	60/30/10	–

The low-density polyethylene (LDPE) was supplied in pellet form by Sasol Polymers, Johannesburg, South Africa. It has an MFI of 7.0 g/10 min (ASTM D-1238), a melting point of 106°C, an average molar mass of 96,000 g mol^{-1}, and a density of 0.918 g cm^{-3}. Sisal fiber was obtained from the National Sisal Marketing Committee in Pietermaritzburg.

Methods

The fibers were cut into ~ 9 mm lengths using a pair of scissors. The fibers were soaked in petroleum ether for 6 h to remove fatty impurities. To ensure easy blending of the fibers and the LDPE, the fibers were washed thoroughly with warm distilled water to remove petroleum ether traces,[35] allowed to air dry at room temperature for at least 4 days and then put in an oven at 60°C for 24 h.

The blends and composites were prepared by weighing according to the desired ratios (Table I) to make up a total mass of 37 g, the mass required to thoroughly mix the different components. The samples were initially mixed in a Brabender Plastograph at 160°C at a screw speed of 15 rpm for 25 min. The samples were then melt pressed at 160°C for 10 min at a pressure of 50 bar into 1-mm-thick sheets.

The differential scanning calorimeter (DSC) used is a Perkin Elmer Pyris-1 DSC from Waltham, MA. Analyses were performed under flowing nitrogen (20 mL min^{-1}). The instument was calibrated using the onset temparatures of melting of indium and zinc standards, as well as the melting enthalpy of indium. Nearly 5–10 mg samples were sealed in aluminium pans, heated from 0 to 160°C at a heating rate of 10°C min^{-1}, and cooled at the same rate to 0°C. For the second scan, the samples were heated and cooled under the same conditions. The onset and peak temperatures of melting and crystallization, as well as the melting and crystallization enthalpies were determined from the second scan.

The thermogravimetric analyzer (TGA) used is a Perkin Elmer TGA7 from Waltham, MA. Analyses were performed under flowing nitrogen at a flow rate of 20 mL min^{-1}. Samples (5–10 mg) were heated from 25 to 600°C at 20°C min^{-1}.

A Hounsfield H5KS universal testing machine from Redhill, United Kingdom was used for the tensile analysis of the samples. The dumbbell samples were stretched at a speed of 50 mm min^{-1} under a cell load of 2500 *N*. The gauge length was 24 mm, the thickness was 1.0 ± 0.1 mm and the width was 4.8 mm. The final mechanical properties were evaluated from five different measurements.

SEM analyses were carried out in a JEOL WIN-SEM-6400 scanning electron microscope from Tokyo, Japan. The probe size was 114.98 nm, the probe current 0.02 nA, the noise reduction 64 Fr and the AC voltage 5.0 keV. The surfaces of the samples were sputter-coated with gold.

RESULTS AND DISCUSSION

The SEM pictures, at two different magnifications, of a fractured surface of an OxWax modified composite at 30% sisal content are illustrated in Figure 2. Although Figure 2(a) shows evidence of fiber pull-out from the LDPE/OxWax matrix, there is also clear evidence of fiber bending, fiber fracture, and intimate contact between the fiber and the matrix. It also seems as if the fiber may be covered by the wax [also see area indicated by arrow in Fig. 2(b)].

The reported DSC heating curves were taken from the second heating scan to eliminate the thermal history. The values of the melting peak temperatures, as well as the experimental and calculated enthalpies, are summarized in Table II. The measured melting enthalpies (ΔH_m^{obs}) were compared with the calculated values (ΔH_m^{calc}). The ΔH_m^{calc} values were determined from the melting enthalpies of pure LDPE and pure wax, and the weight fractions of LDPE and wax in the respective blend composites according to the additive rule in Eq. (1). Here we assume sisal fiber to have no effect on the LDPE and wax crystallization behavior.

$$\Delta H_m^{calc} = \Delta H_{m,PE} w_{PE} + \Delta H_{m,w} w_w$$

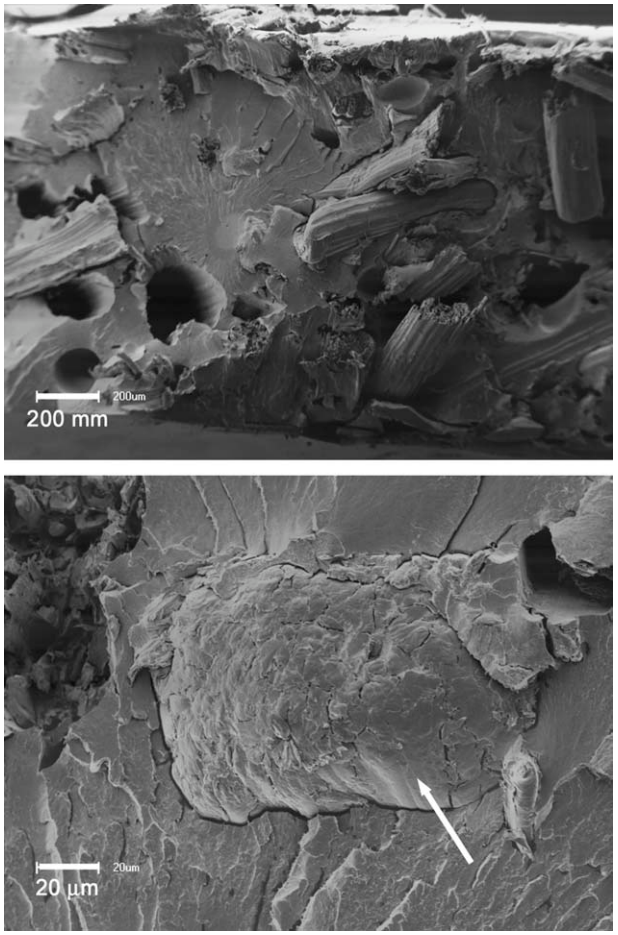

Figure 2 SEM micrographs for 65/30/5 w/w LDPE/sisal/OxWax composites at (a) 100× and (b) 1000× magnification.

where $\Delta H_{m,PE}$, $\Delta H_{m,w}$, ΔH_m^{calc} are the specific enthalpies of melting of PE, wax, and blends, and w_{PE}, w_w are the mass fractions of PE and wax in the blends.

The melting temperature and enthalpy values for pure LDPE and the LDPE/sisal composites with different sisal contents are summarized in Table II. Only one endothermic peak was observed around the melting temperature of LDPE. Generally, there was no change in melting peak temperature with increasing fiber content. The presence of sisal fiber also does not seem to influence the melting enthalpy of the composites, which can be seen from the observed and calculated melting enthalpy values, which were almost the same within experimental error. As expected, the measured enthalpy values decrease, because only LDPE melts, and there are decreasing amounts of LDPE in the samples with increasing sisal content. The fact that there are no changes in the melting temperature, and that the observed and calculated melting enthalpies are almost the same, is an indication that the fiber had very little influence on the crystallization mechanism of LDPE.

The DSC heating curves of the LDPE/OxWax and LDPE/MA-*g*-wax blends are not shown, but the melting temperature and enthalpy values are summarized in Table II. The neat OxWax shows two well-defined separate peaks at 73 and 96°C, and the neat MA-*g*-wax shows peaks at 79 and 105°C. Luyt and Krupa[36] reported that the multiple endothermic peaks of hard paraffin waxes were due to the melting of different molar mass fractions. Only one endothermic peak was seen for the 5% OxWax containing blend, indicating miscibility of LDPE and OxWax at this wax content. However, in the case of the 10% OxWax blend there was an additional peak around the wax melting temperature. This could be attributed to the partial immiscibility of OxWax and LDPE at higher wax contents. The presence of OxWax reduces the melting temperature of LDPE, with relatively no change as the OxWax content increases. It seems as if the molten wax has an influence on the crystal growth mechanism of LDPE during controlled cooling. The introduction of OxWax in LDPE has no significant effect on the melting enthalpy of the blends, probably because the pure wax

TABLE II
DSC Results for LDPE, LDPE/MA-*g*-wax, and LDPE/OxWax Blends, as Well as LDPE/Sisal, LDPE/Sisal/MA-*g*-Wax, and LDPE/Sisal/OxWax Composites

Sample w/w	$T_{p,m}$/°C	ΔH_m^{obs}/J g^{-1}	ΔH_m^{calc}/J g^{-1}
LDPE			
100/0	110.3	53.6	–
LDPE/sisal			
90/10	109.4	49.0	48.2
80/20	110.0	43.7	42.9
70/30	110.0	38.5	37.5
LDPE/OxWax			
95/5	103.5	52.3	53.8
90/10	103.8	52.6	54.0
0/100	75.2[a] 96.5[b]	57.3	–
LDPE/MA-*g*-wax			
95/5	109.0	49.6	57.0
90/10	109.2	52.8	60.3
0/100	105.3[a] 73.0[b]	120.9	–
LDPE/sisal/OxWax			
85/10/5	104.5	50.4	48.4
80/10/10	104.4	49.0	48.6
75/20/5	104.0	41.1	43.1
70/20/10	104.5	32.9	43.2
65/30/5	104.9	25.9	37.7
60/30/10	105.0	24.8	37.9
LDPE/sisal/MA-*g*-wax			
85/10/5	109.0	55.5	51.6
80/10/10	109.0	45.9	55.0
75/20/5	109.9	43.4	46.2
70/20/10	109.4	39.3	49.6
65/30/5/	110.5	36.3	40.0
60/30/10	109.7	31.8	38.2

$T_{p,m}$, ΔH_m^{obs}, and ΔH_m^{calc} are the melting peak temperature, observed melting enthalpy, calculated melting enthalpy. a and b indicate temperatures of two peak maxima in double wax melting peaks.

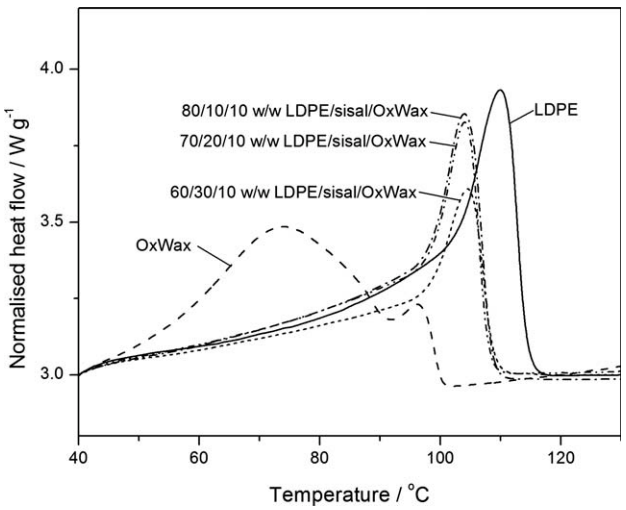

Figure 3 DSC heating curves of pure LDPE and LDPE/sisal/OxWax composites.

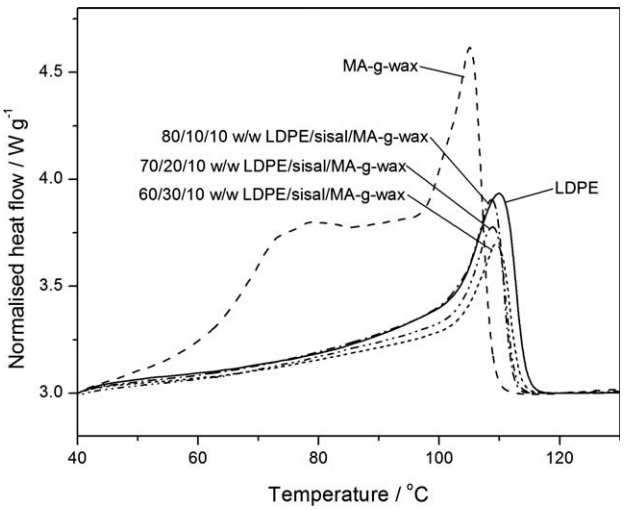

Figure 4 DSC heating curves of pure LDPE and LDPE/sisal/MA-*g*-wax composites.

has a similar melting enthalpy than LDPE. The melting behavior of the LDPE/MA-*g*-wax blends is similar to that of pure LDPE, which suggests possible co-crystallization of PE and wax chains. MA-*g*-wax has a much higher melting enthalpy than pure LDPE (Table II). The observed melting enthalpy values of the blends are lower than the calculated values. This shows that the presence of MA-g-wax lowered the crystallinity of the blends. This is probably the result of the better interaction between LDPE and MA-*g*-wax, which led to better miscibility between these two components, and as a consequence there were fewer wax crystals in the amorphous phase of the LDPE.

The DSC heating curves of LDPE/sisal/OxWax and LDPE/sisal/MA-*g*-wax composites are respectively shown in Figures 3 and 4. There is only one endothermic peak around the melting temperature of LDPE. The melting peak temperatures for the LDPE/sisal/OxWax composites are lower than that of pure LDPE (Fig. 3 and Table II). Although the exact influence of wax on the crystallization behavior of polyethylenes is still unclear, the lower melting temperatures of these samples are probably caused by a change in the crystallization behavior of LDPE in the presence of molten wax. The observed and calculated melting enthalpy values are almost the same for the 10% fiber containing samples, while the differences between the observed and calculated values become bigger with increasing fiber content. This may be the result of the complete coverage of the fibers by OxWax at the lower fiber content, which led to the fibers having little influence on the LDPE crystallization behavior. The increase in differences between the observed and calculated values is difficult to explain, because a reduction in sample crystallinity in the presence of sisal fiber and functionalized wax may be the result of several factors: (i) the extent to which the wax crystallizes around the cellulosic fibers; (ii) the extent to which the wax co-crystallizes with LDPE; (iii) the extent to which the wax crystallizes separately in the amorphous phase of LDPE. It can be seen in Figure 4 that the melting peak temperatures of the composites in the presence of MA-g-wax remained fairly constant within experimental error with increasing sisal and MA-*g*-wax contents. Similar to the OxWax composite systems, the experimentally observed melting enthalpies of the LDPE/sisal/MA-*g*-wax are lower than the calculated enthalpies for all the investigated wax contents, except for the 85/10/5 w/w LDPE/sisal/MA-*g*-wax sample. Similar to the blends, this may be the result of the better miscibility of MA-*g*-wax with the LDPE matrix.

The TGA curves of LDPE, as well as its respective blends and composites, are shown in Figure 5. Both

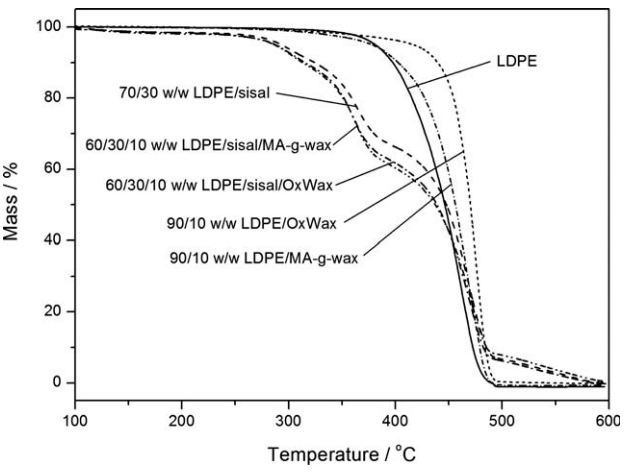

Figure 5 TGA curves of LDPE and its different blends and composites used in this study.

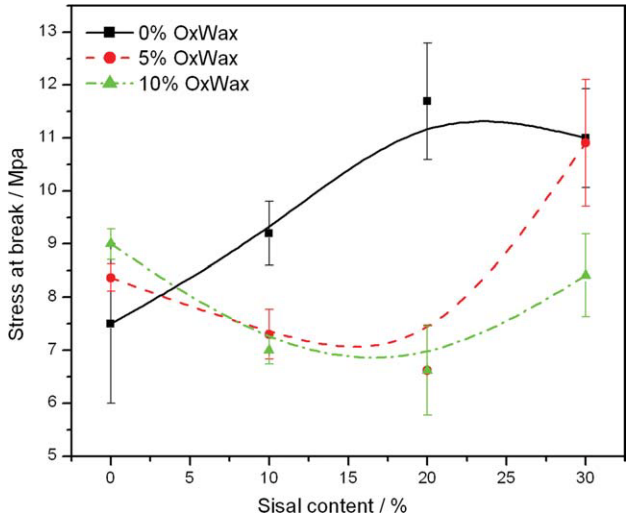

Figure 6 Stress at break as function of sisal content for the LDPE/sisal/OxWax composites. [Color figure can be viewed in the online issue, which is available at wileyonlinelibrary.com.]

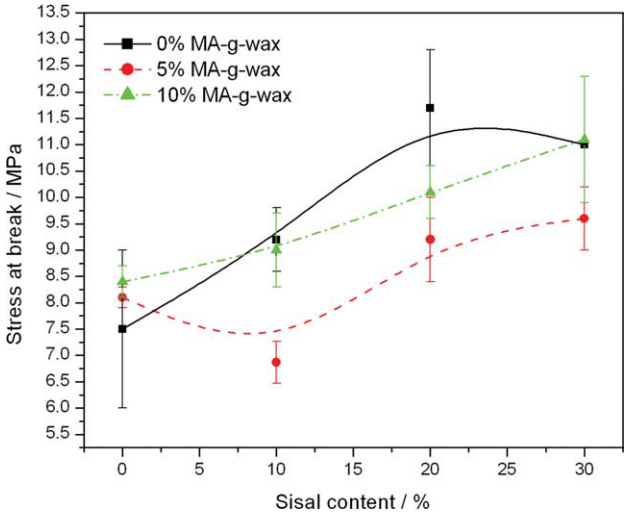

Figure 7 Stress at break as function of sisal content for the LDPE/sisal/MA-*g*-wax composites. [Color figure can be viewed in the online issue, which is available at wileyonlinelibrary.com.]

LDPE/wax blends show better thermal stability than pure LDPE, despite the fact that the unmixed waxes start decomposing at lower temperatures than the pure LDPE (curves not presented). The reason for this is not immediately obvious, but factors that could contribute to this improvement in thermal stability are: (i) protection of the wax chains from the applied heat by the weak thermally conductive and thermally more stable polymer chains, and (ii) inhibition of the diffusion of degradation products through the molten blend, probably because of interaction with the functional groups on the wax chains. The decomposition of LDPE as well as the LDPE/OxWax and LDPE/MA-*g*-wax blends seems to occur in one step, while there clearly are several degradation steps for the LDPE/sisal and LDPE/sisal/wax composites. The step starting at about 100°C for the LDPE/sisal composite is due to the vaporization of moisture from the fiber. The other steps for this composite are due to the thermal depolymerization of hemicellulose and the cleavage of the glycosidic linkages in cellulose, as well as the further breakdown of the decomposition products of the second step, leading to the formation of char. The last step will be the decomposition of LDPE. The TGA curves for the LDPE/sisal/wax composites have shapes similar to that of the LDPE/sisal composite, but the LDPE/sisal/wax composites seem to degrade faster between 270 and 470°C. This is probably the result of the thermally less stable wax chains that interact more strongly with the fiber and that crystallized around the fiber. There does not seem to be a difference between the thermal stabilities of the composites containing the two different waxes.

The stress at break and tensile modulus of all the samples are shown as function of sisal content in Figures 6–9. The effect of OxWax and MA-*g*-wax content on the stress at break is shown in Figures 6 and 7. Samples prepared in the absence of wax show an increase in stress at break for 10 and 20% sisal, with the 20% containing sample showing a maximum value (Fig. 6). Vilaseca et al.[37] investigated the composite system of PP and abaca strands in the absence and presence of maleated polypropylene. They found that the tensile strength at break of the untreated composites increased remarkably with increasing abaca content. They associated this behavior with the mechanical anchoring between the fiber and the matrix, and to the diffusion of the polymer into the fiber. Possible reasons for the decline in

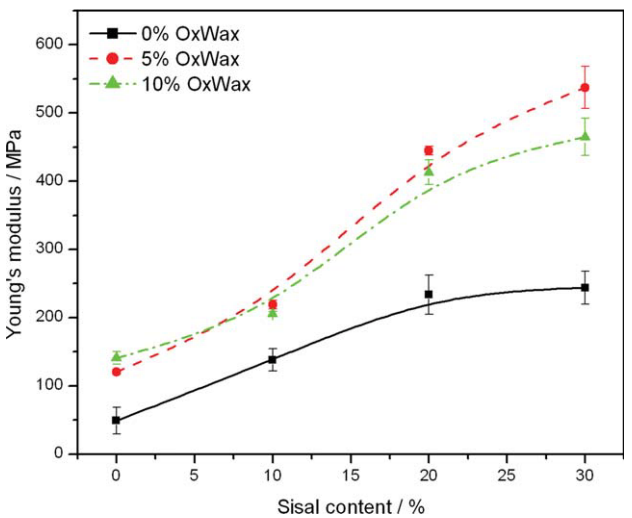

Figure 8 Young's modulus as function of sisal content for the LDPE/sisal/OxWax composites. [Color figure can be viewed in the online issue, which is available at wileyonlinelibrary.com.]

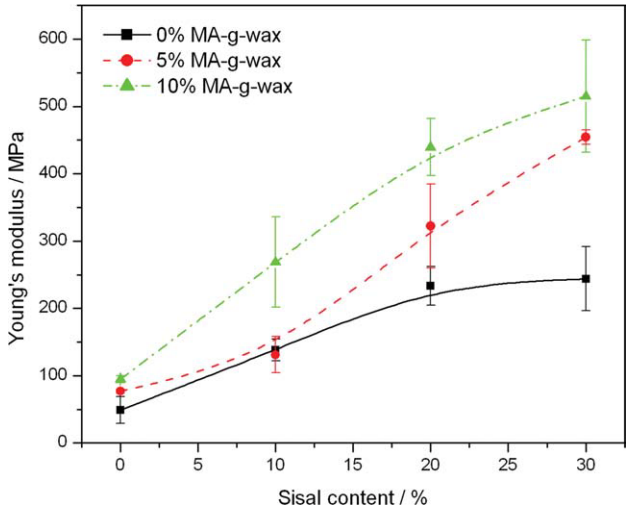

Figure 9 Young's modulus as function of sisal content in the LDPE/sisal/MA-*g*-wax composites. [Color figure can be viewed in the online issue, which is available at wileyonlinelibrary.com.]

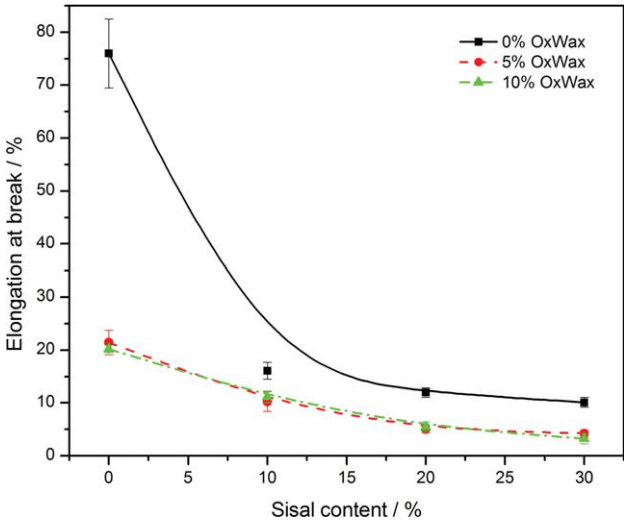

Figure 10 Elongation at break as function of sisal content for the LDPE/sisal/OxWax composites. [Color figure can be viewed in the online issue, which is available at wileyonlinelibrary.com.]

stress at break at high fiber content are: (i) poor interfacial adhesion, which promotes microcrack formation at the interface as well as non-uniform stress transfer because of fiber agglomeration (fiber–fiber contact which results in fiber damage) within the LDPE matrix, and (ii) an increase in the number of voids in the composites that serve as local areas for crack initiation.[38] For both the 5 and 10% OxWax containing samples there is an observable decrease in tensile strength at break with increasing sisal fiber content up to about 15% fiber, with an increase at higher sisal fiber contents (Fig. 6). The initial decrease is probably because (a) at lower fiber contents the fiber is completely covered by wax, and (b) there seems to be a weaker interaction between LDPE and the wax. At higher fiber contents there is not enough wax to completely cover the fibers, and there may be better interaction between the LDPE and the fibers because of mechanical interlocking. This will lead to better stress transfer and increasing tensile strength. Figure 7 shows the stress at break for the MA-*g*-wax containing samples. Generally the tensile strength at break increases with an increase in sisal content. This could be a consequence of MA-*g*-wax having a higher affinity for LDPE and, because the wax was concentrated around the fiber, there is a higher affinity between LDPE and the wax-covered filler.

Figures 8 and 9 show the effect of fiber and wax contents on the Young's modulus values of the samples. For all the composites there is a general increase in Young's modulus with increasing sisal content. Generally, the presence of solid filler increases the Young's modulus of composites. The modulus values for the OxWax containing samples are significantly higher than those of the composites prepared in the absence of wax, and this difference becomes bigger with increasing sisal content. This can be attributed to the higher degree of crystallinity of the OxWax, as can be seen from the DSC results (Table II), and to better stress transfer because of better wetting of the fibers in the presence of OxWax. However, differences in the OxWax content do not show much influence on the modulus values (Fig. 8). In the case of the MA-*g*-wax containing composites (Fig. 9), the Young's modulus increased with both increasing sisal and wax contents, and the differences are also bigger at higher sisal contents. In this case the high modulus could be related to the higher miscibility of MA-*g*-wax with LDPE, as well

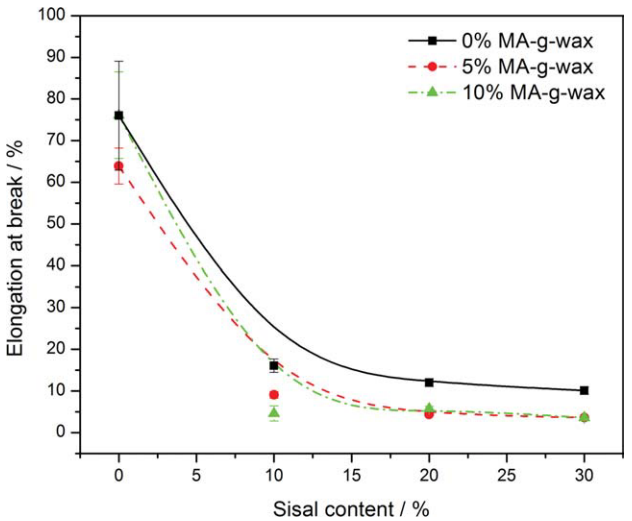

Figure 11 Elongation at break as function of sisal content for the LDPE/sisal/MA-*g*-wax composites. [Color figure can be viewed in the online issue, which is available at wileyonlinelibrary.com.]

as to the wax more effectively covering the sisal fiber at low fiber contents.

The effect of OxWax and MA-*g*-wax contents on the elongation at break are shown in Figures 10 and 11. In Figure 10 it can be seen that the elongation at break decreases with increasing sisal content. This indicates that the presence of fiber in the matrix reduces the ability of the sample to deform by restricting the mobility of the polymer chains, even in the presence of OxWax. Figure 11 shows a general decrease in elongation at break with an increase in sisal fiber content. This is normal for polymers containing rigid fillers, because the fillers act as defect centers that give rise to reduced stress transfer. The presence of OxWax considerably reduced the elongation at break, while the presence of MA-*g*-wax only slightly reduced the elongation at break. In the case of MA-*g*-wax, this could be associated with a better interaction between the polymer and the MA-*g*-wax and therefore better stress transfer. The OxWax behaved differently due to the crystallization of the wax in the amorphous phase of the LDPE, and which formed defect centers in the polymer matrix.

CONCLUSIONS

The purpose of the study was to investigate the effect of functionalized waxes, OxWax and MA-*g*-wax, as compatibilizers on the morphology and properties of LDPE/sisal composites. SEM observations could not conclusively confirm better interaction between the sisal fiber and the LDPE/wax matrix, although there were indications of preferable crystallization of the wax on the surfaces of the sisal fibers.

The differential scanning calorimetry (DSC) results showed that sisal alone did not change the melting or crystallization behavior of LDPE, while the two waxes influenced the melting and crystallization behavior of LDPE in different ways, whether mixed with LDPE alone or in the presence of sisal. The thermal properties seem to be influenced by the fact that the waxes preferably crystallize around the short sisal fibers, and by the fact that the two waxes have different compatibilities with LDPE. The TGA results showed an increase in the thermal stability of the LDPE/wax blends for both waxes, with LDPE/OxWax showing a more significant improvement. The thermal stabilities of the composites were dominated by the low thermal stability of the natural fiber, but the presence of wax further reduced the thermal stabilities of the composites, with both waxes showing similar influence.

The presence of OxWax and MA-*g*-wax similarly influenced the tensile properties of the composites. Both waxes improved the modulus of the compatibilized composites, but in both cases the tensile strengths were worse, probably because of a fairly weak interaction between LDPE and the respective waxes.

References

1. Georgopoulos, S. T.; Tarantili, P. A.; Avgerinous, E.; Andreopoloulos, A. G.; Koukios, E. G. Polym Degrad Stab 2008, 90, 303.
2. Joshi, S. V.; Drazl, L. T.; Mohanty, A. K.; Arora, S. Compos A 2004, 35, 371.
3. Singha, A. S.; Thakur, V. K. Bull Mater Sci 2008, 31, 791.
4. Pracella, M.; Chionna, D.; Anguillesi, I.; Kulinski, Z.; Piorkowska, E. Compos Sci Technol 2006, 66, 2218.
5. Albano, C.; Reyes, J.; Ichazo, M.; Gonzalez, J.; Brito, M.; Moronta, D. Polym Degrad Stab 2002, 76, 191.
6. Albano, C.; Karam, A.; Domĭnguez, D.; Sánchez, Y.; González, J.; Aguirre, O.; Cataño, L. Compos Struct 2005, 71, 282.
7. Colom, X.; Carrasco, F.; Pages, P.; Cañavate, J. Compos Sci Technol 2003, 63, 161.
8. Qui, W.; Endo, T.; Hirotsu, T. Eur Polym J 2006, 42, 1059.
9. George, J.; Bhagawan, S. S.; Thomas, S. Compos Sci Technol 1998, 58, 1471.
10. Joseph, P. V.; Joseph, K.; Thomas, S.; Pillai, C. K. S.; Prasad, V. S.; Groeninckx, G.; Sarkissova, M. Compos A 2005, 34, 253.
11. Barone, J. R. Compos A 2005, 36, 1518.
12. Mohanty, S.; Verma, S. K.; Nayak, S. K. Compos Sci Technol 2006, 66, 538.
13. Yaun, X.; Jayaraman, K.; Bhattacharrya, D. Compos A 2004, 35, 1363.
14. Torres, F. G.; Cubillas, M. L. Polym Test 2005, 24, 694.
15. Mengeloglu, F.; Kabakci, A. Int J Mater Sci 2008, 9, 107.
16. Bengston, M.; Gatenholm, P.; Oksman, K. Compos Sci Technol 2005, 65, 1468.
17. Li, Y.; Hu, C.; Yu, Y. Compos A 2008, 39, 570.
18. Joseph, K.; Thomas, S.; Pavithran, C. Compos Sci Technol 1995, 53, 99.
19. Kaci, M.; Djidjelli, H.; Boukerrou, A.; Zaidi, L. Express Polym Lett 2007, 7, 467.
20. Oksman, K.; Lindberg, H. J Appl Polym Sci 1998, 68, 1845.
21. Lu, J. Z.; Wu, Q.; Negulescu, I. I. J Appl Polym Sci 2005, 96, 93.
22. Hato, M. J.; Luyt, A. S. J Appl Polym Sci 2007, 104, 2225.
23. Li, Y.; Mai, Y-W.; Ye, L. Compos Sci Technol 2000, 60, 2037.
24. Nachtigall, S. M. B.; Cerveira, G. S.; Rosa, S. M. L. Polym Test 2007, 26, 619.
25. Nygård, P.; Tanem, B. S.; Karlsen, T.; Branchet, P.; Leinsvang, B. Compos Sci Technol 2008, 68, 3418.
26. Yuan, X.; Jayaraman, K.; Bhattacharyya, D. Compos A 2004, 35, 1363.
27. Mohanty, S.; Nayak, S. K. Mater Sci Eng A 2007, 443, 202.
28. Fung, K. L.; Li, R. K. Y.; Tjong, S. C. J Appl Polym Sci 2002, 85, 165.
29. Joseph, P. V.; Rabello, M. S.; Mattoso, L. H. C.; Joseph, K.; Thomas, S. Compos Sci Technol 2002, 62, 1357.
30. Dikobe, D. G.; Luyt, A. S. J Appl Polym Sci 2007, 104, 3206.
31. Harper, D.; Wolcott, M. Compos A 2004, 35, 385.
32. Mahfuz, A.; Adnan, A.; Rangari, V. K.; Jeelani, S.; Jang, B. Z. Compos A 2004, 35, 519.
33. Krump, H.; Alexy, P.; Luyt, A. S. Polym Test 2005, 24, 129.
34. Novák, I.; Krupa, I.; Luyt, A. S. J Appl Polym Sci 2006, 100, 3069.
35. Mokoena, M. A.; Djoković, V.; Luyt, A. S. J Mater Sci 2004, 39, 3403.
36. Luyt, A. S.; Krupa, I. Thermochim Acta 2008, 467, 117.
37. Vilaseca, F.; Valadez-Gonzalez, A.; Herrera-Franco, P. J.; Pélach, M. À.; López, J. P.; Mutjé, P. Bioresource Technol 2010, 101, 385.
38. Ruksakulpiwat, Y.; Suppakarn, N.; Sutapun, W.; Thomthong, W. Compos A 2007, 38, 590.